Shear-Wave Velocity Characterization of the USGS Hawaiian Strong-Motion Network on the Island of Hawaii and Development of an NEHRP Site-Class Map

by Ivan G. Wong, Kenneth H. Stokoe II, Brady R. Cox, Jiabei Yuan, Keith L. Knudsen, Fabia Terra, Paul Okubo, and Yin-Cheng Lin

Abstract   To assess the level and nature of ground shaking in Hawaii for the purposes of earthquake hazard mitigation and seismic design, empirical ground-motion prediction models are desired. To develop such empirical relationships, knowledge of the subsurface site conditions beneath strong-motion stations is critical. Thus, as a first step to develop ground-motion prediction models for Hawaii, spectral-analysis-of-surface-waves (SASW) profiling was performed at the 22 free-field U.S. Geological Survey (USGS) strong-motion sites on the Big Island to obtain shear-wave velocity (V_S) data. Nineteen of these stations recorded the 2006 Kiholo Bay moment magnitude ($\mathbf{M}$) 6.7 earthquake, and 17 stations recorded the triggered $\mathbf{M}$ 6.0 Mahukona earthquake. V_S profiling was performed to reach depths of more than 100 ft. Most of the USGS stations are situated on sites underlain by basalt, based on surficial geologic maps. However, the sites have varying degrees of weathering and soil development. The remaining strong-motion stations are located on alluvium or volcanic ash. V_{S30} (average V_S in the top 30 m) values for the stations on basalt ranged from 906 to 1908 ft/s [National Earthquake Hazards Reduction Program (NEHRP) site classes C and D], because most sites were covered with soil of variable thickness. Based on these data, an NEHRP site-class map was developed for the Big Island. These new V_S data will be a significant input into an update of the USGS statewide hazard maps and to the operation of ShakeMap on the island of Hawaii.

Introduction

On 15 October 2006, the island of Hawaii was struck by two earthquakes of moment magnitudes ($\mathbf{M}$) 6.7 and 6.0 (Earthquake Engineering Research Institute, 2006; Fig. 1). The Kiholo Bay mainshock occurred at a depth of 39 km and provided the largest suite of strong-motion records ever produced for an earthquake in Hawaii and the best opportunity to understand the processes of strong ground shaking in the region. The mainshock is also among the largest events to have occurred in Hawaii since written records have been maintained. The shallower $\mathbf{M}$ 6.0 Mahukona earthquake, triggered 7 minutes after the mainshock, occurred at a depth of 19 km. For many, the Kiholo Bay earthquake served as a reminder that Hawaii is not only volcanically but seismically active, and it is exposed to a significant seismic hazard. Klein et al. (2001) indicate that the Big Island possesses one of the highest levels of seismic hazards in the United States. Although no deaths or serious injuries were reported in the Kiholo Bay earthquake, damage estimates exceeded

$200 million, resulting in the declaration of the Kiholo Bay event as a major disaster area by the U.S. government. Most of the damage was on the islands of Hawaii and Maui and was predominantly nonstructural (Earthquake Engineering Research Institute, 2006). Limited structural damage occurred to older, weaker buildings, including Hawaii's unique post-and-pier and single-wall buildings. Over 1800 individual residences were damaged to varying degrees or one of every 25 homes on the Big Island (Earthquake Engineering Research Institute, 2006).

The mainshock was recorded by 19 strong-motion instruments operated on the Big Island by the U.S. Geological Survey (USGS) as part of the Hawaiian Strong Motion Network (Fig. 1; Table 1) and seven distant stations on Maui and Oahu (Stephens et al., 2007). In addition to the mainshock, the $\mathbf{M}$ 6.0 Mahukona event and a deep $\mathbf{M}$ 5.0 Puako aftershock were recorded on 17 and 13 stations, respectively. Mainshock peak horizontal ground accelerations (PGAs)
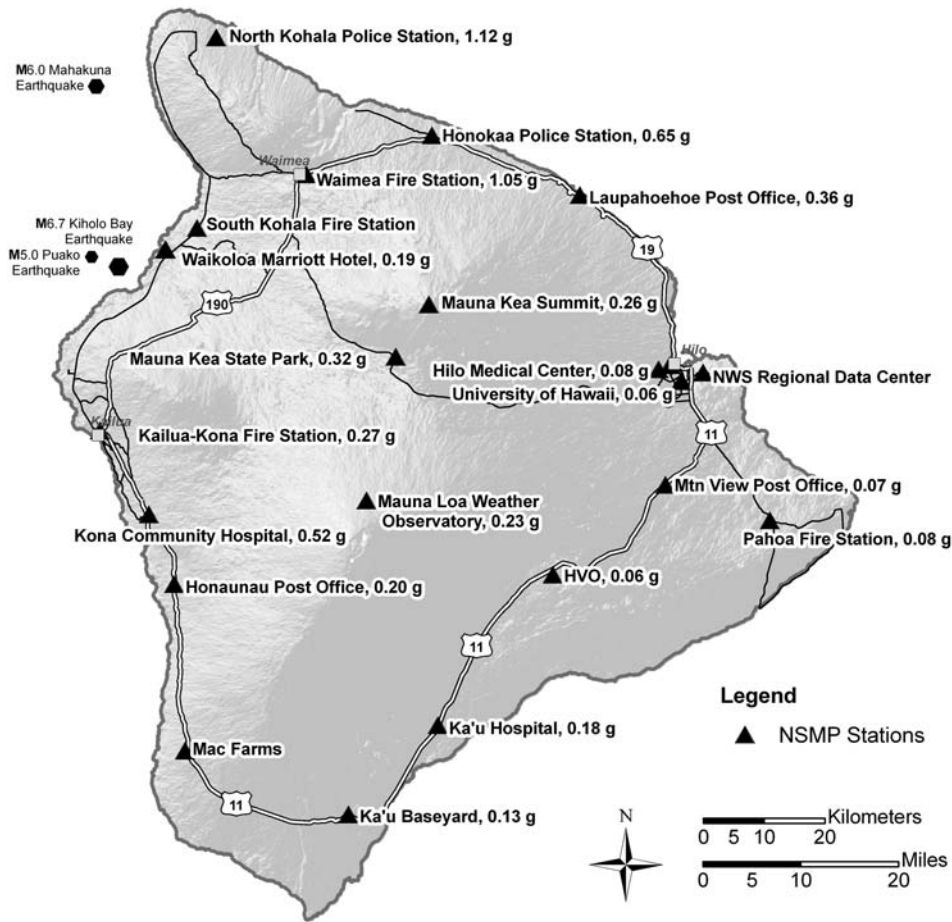
Figure 1.   USGS strong-motion stations and recorded PGAs from the 2006 **M** 6.7 Kiholo Bay mainshock.

Table 1
PGA Values Recorded in the 2006 Kiholo Bay *M* 6.7 and Mahukona *M* 6.0 Earthquakes

Station Name	Hypocentral Distance to Kiholo Bay Mainshock (km)	PGA (*g*)	Hypocentral Distance to Mahukona Event (km)	PGA (*g*)
Waikoloa Marriott Hotel, Anaehoomalu	39.5	0.19	31.6	0.17
Kailua-Kona Fire Station	46.9	0.27	56.5	0.06
Waimea Fire Station	50.9	1.05	40.3	0.17
Kona Community Hospital, Kea Lakekua	55.4	0.52	70.2	0.03
North Kohala Police Station, Kapaau	56.8	1.12	29.1	0.26
Mauna Kea State Park	59.2	0.32	65.9	0.09
Mauna Kea Summit	62.4	0.26	65.8	0.02
Honaunau Post Office	64.4	0.20	81.7	0.05
Mauna Loa Weather Observatory	66.0	0.23	80.5	0.04
Honokaa Police Station	66.7	0.65	57.9	0.03
Laupahoehoe Post Office	84.0	0.36	82.3	0.02
Hawaiian Volcano Observatory (HVO)	93.2	0.06	108.7	0.02
Hilo Medical Center	95.9	0.08	103.2	0.01
USDA Laboratory, Hilo	97.4	0.24	104.5	0.03
Ka'u Hospital, Pāhala	97.5	0.18	117.5	0.03
University of Hawaii, Hilo	99.5	0.06	107.3	0.01
Mountain View Post Office	101.7	0.07	–	–
Ka'u Baseyard, Waiohinu	103.2	0.13	–	–
Pahoa Fire Station	118.6	0.08	130.8	0.01

PGA values from Stephens *et al.* (2007). Events were not recorded at Mac Farms (Honomalino), South Kohala Fire Station (Kamuela), and NWS Data Regional Center (Hilo), which were installed after the 2006 earthquakes. Mahukona earthquake was not recorded at the Mountain View Post Office and Ka'u Baseyard.

ranged up to 1.12 g ($g = 980$ cm/s^2) at the North Kohala Police Station (C. Stephens, USGS, written communication, 2007) (Fig. 1; Table 1). The Waimea Fire Station recorded 1.05 g. Such high PGAs are surprising given the depth of the earthquake. The highest recorded PGA for the Mahukona event was 0.26 g also at the North Kohala Police Station (Table 1).

To be able to utilize the strong-motion data, knowledge of the subsurface site conditions beneath the USGS stations is required. The subsurface geology, and more importantly, the shear-wave velocity (V_S) structure beneath the USGS stations have generally been unknown to date, although the vast majority of stations were installed between 1976 to 1980. Munson and Thurber (1997) measured V_S at three of the current stations using seismic refraction but only to depths of 3 to 5 m. V_S information to a depth of at least 30 m (100 ft) is invaluable to develop Hawaii-specific ground-motion prediction equations, to verify the appropriateness of the ground-motion models being used in the state hazard maps produced by the USGS and in site-specific hazard analyses for engineering design.

The ground-motion prediction models that have been used in the state hazard maps developed by the USGS as part of the National Hazard Mapping Project (Klein *et al.*, 2001) included only one model based on Hawaiian strong-motion data. The relationship by Munson and Thurber (1997) was developed from strong-motion data of Hawaiian earthquakes (22 events, **M** 4.0 to 7.2, 51 PGA values), but for shallow crustal events and for PGA only. They classified sites as either basalt or ash. The USGS used the Youngs *et al.* (1997) model for deep earthquakes (> 20 km), although the model was developed for Wadati-Benioff zone events because no ground-motion prediction equations for deep Hawaiian earthquakes were available at the time.

Very recently, Atkinson (2010) has developed a model for both shallow (depth < 20 km) and deep earthquakes (35 to 40 km) using the referenced empirical approach and the strong-motion database including the 2006 earthquakes. Our V_S database was not available at the time Atkinson (2010) was developing her model, but she has evaluated it subsequently with our database. We are currently developing a relationship for deep earthquakes using the stochastic point-source ground-motion numerical modeling approach calibrated with the available deep earthquake strong-motion data.

To obtain V_S information beneath the 22 USGS free-field strong-motion sites on the Big Island, spectral-analysis-of-surface-waves (SASW) surveys were performed by the University of Texas, Austin (UT); the University of Arkansas; and URS Corporation (Wong *et al.*, 2008). The following describes the results of those surveys and the development of an NEHRP site-class map for the island of Hawaii, which is critical input into both building code-based and site-specific seismic design. V_S information will also be an important input into the operation of ShakeMap on the Big Island. Note a mixture of English and metric units are used in this paper. The SASW surveys and data analyses were performed using feet, so the SASW results are reported in those units. All other units are metric.

Seismotectonic and Geologic Setting

The Big Island is one of the most seismically active regions in the United States, with seismicity and seismic hazard on par with coastal California, although it is far from a tectonic plate boundary. Most of the seismicity is at least indirectly related to volcanism, explaining why 43 **M** > 6 earthquakes have occurred on the volcanically active Big Island since 1868, whereas only 8 such events have occurred in the rest of the Hawaiian Island chain (Klein *et al.*, 2001). Earthquakes in Hawaii fall into several categories. Most are concentrated under the active volcanoes of Mauna Loa, Kilauea, and Hualalai and are related to the migration and intrusion of magma under and into the volcanoes. Small earthquakes caused by migration of magma often occur in shallow swarms, especially preceding an eruption. Hundreds of such earthquakes may occur in the days leading up to an eruption, but they rarely cause significant damage. In addition, many of Hawaii's largest earthquakes are related to magma injection along major rift zones that flank the active volcanoes. Intrusions of magma into the rifts introduce compressive stresses that are stored in the adjacent rock to be released periodically in large earthquakes. These earthquakes are triggered when the seaward block flanking the rift zone slips laterally on a subhorizontal décollement away from the rift as it makes way for intruding magma and relieves the stored stress (Klein *et al.*, 2001). These décollements are typically 8 to 10 km deep and lie at the boundary between old oceanic crust and the relatively newly emplaced volcanic edifice. Two of Hawaii's largest historical earthquakes, the 1975 **M** 7.2 Kalapana earthquake and the 1868 **M** 7.9 Ka'u district earthquake, both occurred as a result of such décollement slip. The largest historical Hawaiian earthquake was the 2 April 1868 earthquake, which occurred in the Ka'u district along Mauna Loa's southeastern flank, and had an estimated magnitude of **M** 7.9.

Another category of earthquakes in Hawaii is indirectly related to volcanism and includes earthquakes that occur primarily in the upper mantle (i.e., 20 to 60 km deep). These earthquakes tend to occur in a ring surrounding the island and are probably caused by fracturing in response to lithospheric flexure under the weight of the overlying volcanic edifice. Earthquakes of this type include the 1938 **M** 7 Maui, the 1973 **M** 6.2 Honomu, and the 2006 Kiholo Bay earthquakes.

Based on the USGS Hawaii state hazard maps, PGA values for a 2% exceedance in 50 years (return period of 2475 years) on the Big Island range up to 1.8 g on the South Coast (Klein *et al.*, 2001). In the area of Kiholo Bay, the PGAs are up to 0.8 g. The state hazard maps are for an NEHRP B/C site class, that is, V_{S30} (average V_S in the top 30 m) of 760 m/s

(2493 ft/s). As discussed later, 2493 ft/s is higher than any V_{S30} value measured on the Big Island.

The island of Hawaii is composed of eruptive products from five distinct volcanoes; they are, from oldest to youngest, Kohala, Hualalai, Mauna Kea, Mauna Loa, and Kilauea (Wolfe and Morris, 1996). Kilauea and Mauna Loa are very active shield-stage volcanoes whose lava is generally composed of tholeiitic basalt. Hualalai, Mauna Kea, and Kohala are all capped by postshield lavas, which are more alkalic than the shield-stage basalt.

Major geologic map units and their ages on the Big Island include Puna (Holocene), Hilina (Pleistocene), Ka'u (Holocene and Pleistocene), Kahuku (Pleistocene), and Ninole (Pleistocene) basalts of Kilauea; the Hualalai basalt (Holocene and Pleistocene); Laupahoehoe (Holocene and Pleistocene), Hamakua (Pleistocene), Hawi (Pleistocene), and Polohu (Pleistocene) volcanics of Mauna Kea, Pāhala Ash, and smaller landslide deposits, alluvium and colluvium, eolian deposits, slope deposits, and artificial fill (Wolfe and Morris, 1996). Only the Pāhala Ash is found in any abundance. The ash is a deeply weathered ash that can be as much as 15 m thick and predates the earliest Holocene lavas on Kilauea and Mauna Loa. Detailed descriptions of these units are presented on Table 2.

SASW Methodology

The V_S structure at each site was measured using the SASW technique. The SASW method is widely accepted and has been applied to numerous soil and rock sites (Stokoe *et al.*, 1994, 2004). In particular, the SASW method has often been applied to the problem of characterizing materials for near-surface site response analysis (Rosenblad *et al.*, 2001; Wong and Silva, 2006).

The SASW methodology is a nondestructive and nonintrusive seismic method. It utilizes the dispersive nature of Rayleigh-type surface waves propagating through a layered material to estimate the V_S profile of the material (Stokoe *et al.*, 1994). In this context, dispersion arises when surface-wave velocity varies with wavelength or frequency. Dispersion in surface-wave velocity arises from changing stiffness properties of the soil and rock layers with depth. This phenomenon is illustrated in Figure 2 for a multilayered solid. A high-frequency surface wave, which propagates with a short wavelength, only stresses material near the exposed surface and thus only samples the properties of the shallow, near-surface material (Fig. 2b). A lower-frequency surface wave, which has a longer wavelength, stresses material to a greater depth and thus samples the properties of both shallower and deeper materials (Fig. 2c). Spectral analysis is used to separate the waves by frequency and wavelength to determine the experimental (field) dispersion curve for the site via phase unwrapping. An effective/superposed-mode inversion that takes into account ground motions induced by fundamental and higher-mode surface waves as well as body waves (i.e., a full wavefield solution) is then used to match theoretically

the field dispersion curve with a 1D layered system of varying layer stiffnesses and thicknesses (Joh, 1996). The 1D V_S profile that generates a dispersion curve that best matches the field dispersion curve is selected as the site profile. The 1D geometry is an important assumption. Departures from this geometry, such as when velocity layers are dipping, can result in considerable variability in the dispersion curves and hence multiple interpretations.

SASW measurements involve generating surface waves at one point on the ground surface and recording them as they pass by pairs of receivers at multiple locations. All measurement points are arranged along a single radial path from the source. Successively longer spacings between the receiver pairs and between the source and first receiver in the pair are typically used to measure progressively longer wavelengths. The distance between the source and first receiver in the pair (d) is typically kept equal to the distance between receivers in the pair in order to mitigate near-field effects. Measurements are performed with several (typically seven or more) sets of source-receiver pair spacings. Phase plots from surface waves propagating between each receiver pair are recorded. From each phase plot, the phase velocity of the surface wave can be calculated at each frequency from (Joh, 1996):

$$V_R = f \times \frac{360}{\phi} \times d, \qquad (1)$$

where V_R is the phase velocity in ft/s or m/s, f is the frequency in Hertz (cycles/s), ϕ is the phase angle in degrees (at frequency f), and d is the distance between the receivers in the same length units used to represent V_R. From this calculation, a plot of phase velocity versus frequency, called an individual dispersion curve, is generated. This procedure is repeated for all receiver spacings used at the site and typically involves significant overlapping in the dispersion data between adjacent receiver sets. The individual dispersion curves from all receiver spacings are combined into a single composite dispersion curve called the experimental or field dispersion curve, which contains literally hundreds of individual dispersion measurements. The composite dispersion curve is compacted by using a combined polynomial fit and a moving average analysis procedure. Once the compacted dispersion curve is generated, an iterative forward modeling procedure is used to create a theoretical dispersion curve to match the observed curve (Joh, 1996). The stiffness profile that provides the best match to the observed dispersion curve is presented as the V_S profile at the site.

The SASW method is cost effective and well-suited for *in situ* testing. The method has been validated at numerous sites in blind comparisons. For example, downhole, OYO suspension, and SASW V_S profiles were compared at Yucca Mountain, Nevada (Stokoe *et al.*, 2003), and Imperial Valley, California (Lin *et al.*, 2008); the results indicated generally good agreement even though the techniques are characterizing different volumes of the subsurface. Both downhole and

Table 2
Island of Hawaii Site Response Units and NEHRP Site Classes

Map Unit*	N[‡]	V_{S30} (ft/s)					NEHRP Site Class[†]	Notes
		Min	Max	Log Mean	Median	±σ		
Basalt	19	890	1902	1312	1365	257	C or D	Includes all basalt/lava units (including lava flows, scoria cones, littoral deposits, spatter or tuff cones, cinder cones, lava domes). About 75 geologic map units are included in this category.
Ash/tephra	2	437	1430	NA	NA	NA	D or E	Includes map unit Qt and map units from each volcano. Low on west flank of Mauna Kea, comprises unconsolidated, crossbedded, very fine grained to fine grained dune sand and loess blankets interpreted as deposits of wind-reworked ash derived from eruptions at vents of the Laupāhoehoe Volcanics (units Qlcy, Qlc, Qlbc) (Wolfe and Morris, 1996; Porter, 1997). Deeply weathered elsewhere on Island of Hawai'i where encompassing the Pāhala Ash, a stratigraphic name applied by Wolfe and Morris (1996) to both primary and reworked tephra-fall deposits that originated from Kīlauea, Mauna Loa, Mauna Kea, and perhaps Kohala volcanoes. Sherrod *et al.* (2007) reserve the name Pāhala Ash for deposits on the south side of the Island. Younger tephra of Kīlauea has been mapped as units within encompassing volcanic formations; for example, Keanakāko'i Ash Member is labeled as ash beds of age 200 to 500 yr within the Puna Basalt (unit Qpa4) (Sherrod *et al.*, 2007).
Alluvium	1	1176	1176	NA	NA	NA	D or E	Unconsolidated deposits of silt, sand, and gravel along streams and in valley bottoms (Sherrod *et al.*, 2007). Includes interlayered fluvial, eolian, debris-flow, and tephra-fall deposits on south flank of Mauna Kea.
Glacial deposits	0	—	—	—	—	—	C or D	Till and outwash on Mauna Kea (Sherrod *et al.*, 2007).
Artificial fill	2	1250	1439	NA	NA	NA	D or E	Manmade fill forming piers and harbor breakwaters along coastline (Sherrod *et al.*, 2007).[§]
Landslide deposits	0	—	—	—	—	—	C or D	Some deposits incorporated preexisting volcanic ash deposits, which locally contribute high proportion of matrix, as in the Wood Valley area on south flank of Mauna Loa (Sherrod *et al.*, 2007).
Sand dunes	0	—	—	—	—	—	D	Map unit Qdy. Unconsolidated, mostly coralline sand forming eolian sheets and dunes, found chiefly adjacent to beach deposits. On Kīlauea volcano, comprises black glassy and lithic sand reworked downwind onto the volcano's southwest rift zone from 200 to 500-yr-old tephra deposits in the summit area (Sherrod *et al.*, 2007).

*Map units are from Sherrod *et al.* (2007).

[†]NEHRP site classes based on V_{S30} (ft/s) either directly measured or inferred; A, $V_{S30} > 5000$; B, $2500 < V_{S30} < 5000$; C, $1200 < V_{S30} < 2500$; D, $600 < V_{S30} < 1200$; E, $V_{S30} < 600$

[‡]Number of SASW measurements.

[§]Two measurements were made at Kawaihae Harbor where the fill is only about 10 ft thick. The underlying units are coralline sand deposits about 30 to 60 ft thick and basalt.

suspension techniques measure the volume immediately near the borehole, and SASW characterizes the volume below the survey between the source and receivers. The 1D profile resulting from SASW is a global average over the measured volume of the subsurface that has been measured at frequencies that are generally at the bandwidth of most engineering relevance of 1 to 10 Hz.

SASW Survey Results

Until the present study, only a few shallow cone penetrometer test measurements to infer V_S in soft soils have been made on the Big Island. The SASW surveys took place from 7 to 17 January 2008. The 22 free-field strong-motion sites surveyed are shown in Figure 1. Most of the sites are fire
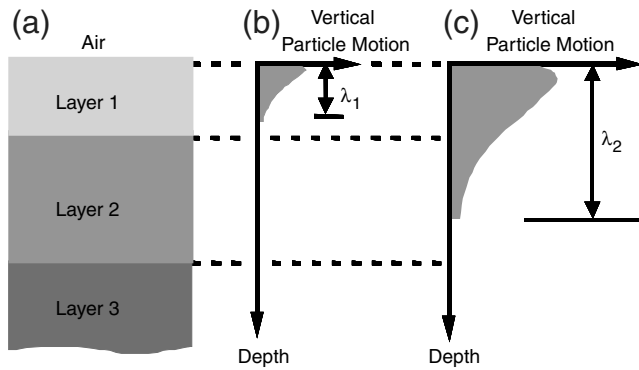
Figure 2. Illustration of surface waves with different wavelengths sampling different materials in a layered system, which results in dispersion in wave velocities: (a) material profile; (b) shorter wavelength, λ_1; and (c) longer wavelength, λ_2.

stations, police stations, hospitals, or post offices. Surveys were generally performed within 100 ft of the location of the USGS strong-motion instrument. For a few sites, this was not possible due to lack of space to perform the surveys so the distance was as much as 200 ft.

Active seismic sources are required for the SASW surveys. A sledgehammer was used for the shorter wavelengths, λ, less than about 50 ft. The larger source used to create wavelengths up to about 600 ft long in this study was the National Science Foundation's Network for Earthquake Engineering Simulation (NEES) mobile vibrator called Thumper (Fig. 3). Thumper, housed and operated by the University of Texas, is a moderate- to high-frequency vibrator. Some important characteristics of Thumper are: (1) mounted on a Ford F650 truck, (2) total weight of about 10,000 kg, and (3) two vibrational orientations (field transformable in a few hours), vertical or horizontal. The maximum force output is about 27 kN over the frequency range of 17 to 225 Hz with the output decreasing outside this frequency band. The relatively low-force output (27 kN) also makes Thumper an excellent vibrator for testing in urban environments where disturbance or possible damage to existing above-ground and below-ground facilities might occur.

In the Hawaii surveys, the full output of Thumper was used in the SASW surveys. A stepped sine excitation was used to collect the surface-wave data at all sites. During this excitation, frequencies from about 200 to 2 Hz were stepped through over a time span of several minutes. The dwell time at low frequencies was greater than at high frequencies to increase the signal-to-noise ratio.

An example composite field dispersion curve collected on the Big Island is presented in Figure 4a. These data were collected at the Pahoa Fire Station using a sledgehammer source with receiver-to-receiver spacings of 6, 12, 15, and 30 ft and Thumper as the source with receiver-to-receiver spacings of 25, 50, 75, 100, 150, and 200 ft using 102 points. The theoretical dispersion curve and its fit to the compacted curve developed in the forward modeling process are shown in Figure 4b. The composite field dispersion curve is

Figure 3. (a) SASW survey in the parking lot at the Hawaiian Volcano Observatory (HVO). Recording and analysis van is in the foreground and Thumper in the far background. (b) Thumper at the top of Mauna Kea. Mauna Loa is in the background.

composed of 3196 data points that cover a frequency range from about 10 to 200 Hz. This frequency range corresponds to a wavelength range of 2.4 to 240 ft. The goodness-of-fit between the theoretical and compacted dispersion curves is represented by the root mean square (rms) error in Figure 4b and by the mean (μ) and standard deviation (σ) of $\Delta V_R / V_R$ in Figure 4c, where V_R is from the compacted dispersion curve, and ΔV_R is the phase velocity difference between the compacted dispersion curve and theoretical dispersion curve at the same frequency. In this case, the rms error is 59.4 ft/s, and the μ and σ are -0.5% and 5.6%, respectively. Typical values found for the 22 sites are rms errors (for V_R) ranging from about 30 to 180 ft/s, μ ranging from -0.4% to 0.5%, and σ ranging from 3.3% to 6.5%.

In terms of the resolution in the V_S profiles, the resolution decreases with depth for all nonintrusive, surface-wave-based methods. For SASW testing on the Big Island, consider the V_S profile of the Pahoa Fire Station. This profile consists of nine layers, with the thickness increasing with depth from 1 ft for the top layer to 50 ft for the eighth layer (Fig. 5).
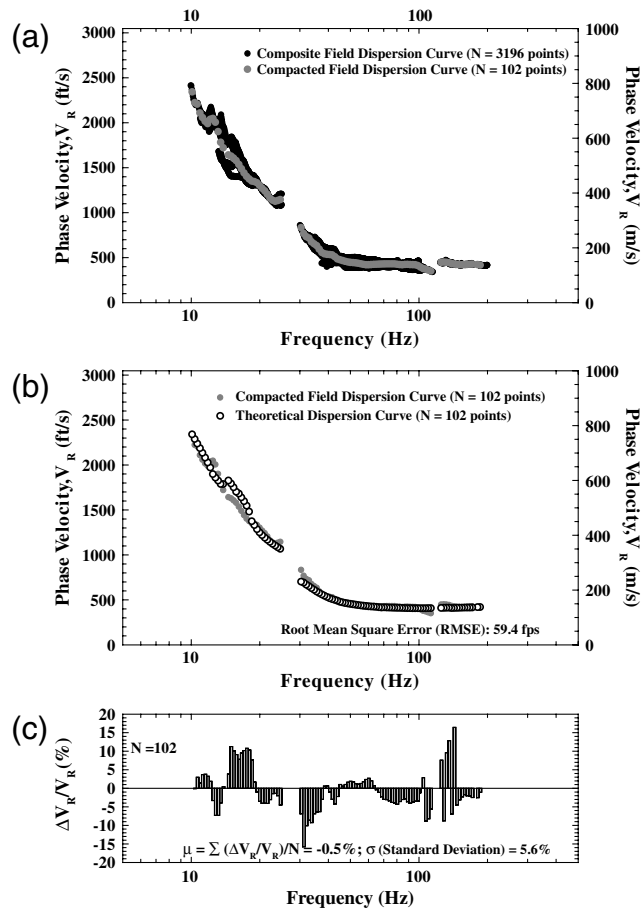
Figure 4. SASW forward modeling process and goodness-of-fit evaluation for the survey at the Pahoa Fire Station: (a) developing the compacted field dispersion curve, (b) fitting the compacted dispersion curve with a theoretical dispersion curve, and (c) determining the mean (μ) and σ of the best fit.

The ninth layer includes the half-space, but only 20 ft of the half-space is presented because the V_S profile is shown only to a depth equal to 0.5 times the maximum wavelength in the composite field dispersion curve. This criterion is used so that the resolution of V_S in the lower portion of the profile is within ±10% to ±15%.

To demonstrate this resolution, consider Figure 5a,b, where the value of V_S in layer 5 has been varied by ±10% from the original best-fit profile. As seen in Figure 5b, these ±10% changes to layer 5 result in theoretical dispersion curves that no longer fit the compacted field dispersion curve. As such, the true V_S for layer 5 is well within 10% in the forward modeling process, and resolution is expected to be even better for the shallower layers. Similarly, in Figure 5c,d, the V_S of layer 8 has been varied by ±10% from the original best-fit profile. In this case, the fit of the original theoretical dispersion curve is still better than the varied profile, indicating that the original V_S profile can be considered, in general terms, to be within 10% of the true V_S value in that depth range over that lateral distance tested. These results are typical of the 22 sites tested on the Big Island.

One of the benefits of SASW is that velocity inversions can be detected. However, the ability to detect these inversions depends on the relative stiffness contrast as well as the inverse layer thickness and its absolute depth below the surface. If a velocity inversion is detected at the site, it will be visible in the experimental dispersion curve, so you will know it is present in the data even before the inversion process. The V_S profiles presented herein were not developed simply by setting a predetermined number of layers and letting an automated inversion find the best solution. An iterative forward modeling procedure was used to visually determine a good fit to the data by varying the number and thicknesses of layers. Then an automated inversion was used to refine this visually fit model slightly.

The V_S profiles for the 22 surveys at the strong-motion sites are shown in Figures 6 through 11. The profiling depths ranged from 100 to 318 ft (Table 3). For about 1/3 of the sites, the profiling depth was 124 ft or less. In these cases, the shallower profiling depths resulted from one or more of the following: (1) the available space at the site was insufficient for the longer arrays (source to farthest receiver of 400 to 600 ft) required to profile deeper, (2) there was a significant velocity jump (increase of 40% or more) in the top 100 ft, and (3) there was a substantial thickness (40 ft or more) of soft soil ($V_S < 500$ ft/s) in the upper portion of the site.

In the forward modeling of each field dispersion curve, the depth to the water table (10 to 140 ft) was estimated based on the surrounding topography and elevation relative to the ocean. *P*-wave refraction surveys were tried at three sites to detect the water table. However, it was not found to be successful for several reasons. The authors have found that from a practical standpoint, the more variable the near-surface layering (shallow inversions, gradual stiffness contrasts, etc.), the more difficult it is to analyze the data to locate the water table. Even if strong trends in the wave arrivals are detected, hidden layer effects can mask the true water table depth. Furthermore, the receivers must be placed directly on the native soil and not on asphalt (as in a parking lot), or the direct wave arrival will always be fastest. Many of the test locations required the SASW surveys through a thin layer of asphalt.

Sensitivity analyses indicate that V_S profiles are not sensitive to the water table depth once reasonable estimates are included in the modeling process (Wong *et al.*, 2011). Changing the depth to the water table by a factor of 2 at all 22 stations results in 0.0% difference in V_{S30} at 19 stations and at most 4.4% at the Hawaiian Volcano Observatory (HVO).

Geotechnical Site Characterization

To estimate general categories of geotechnical materials within each profile, the V_S-depth profiles were subdivided and grouped according to relative trends expected for various geotechnical materials. The template of V_S-depth trends used
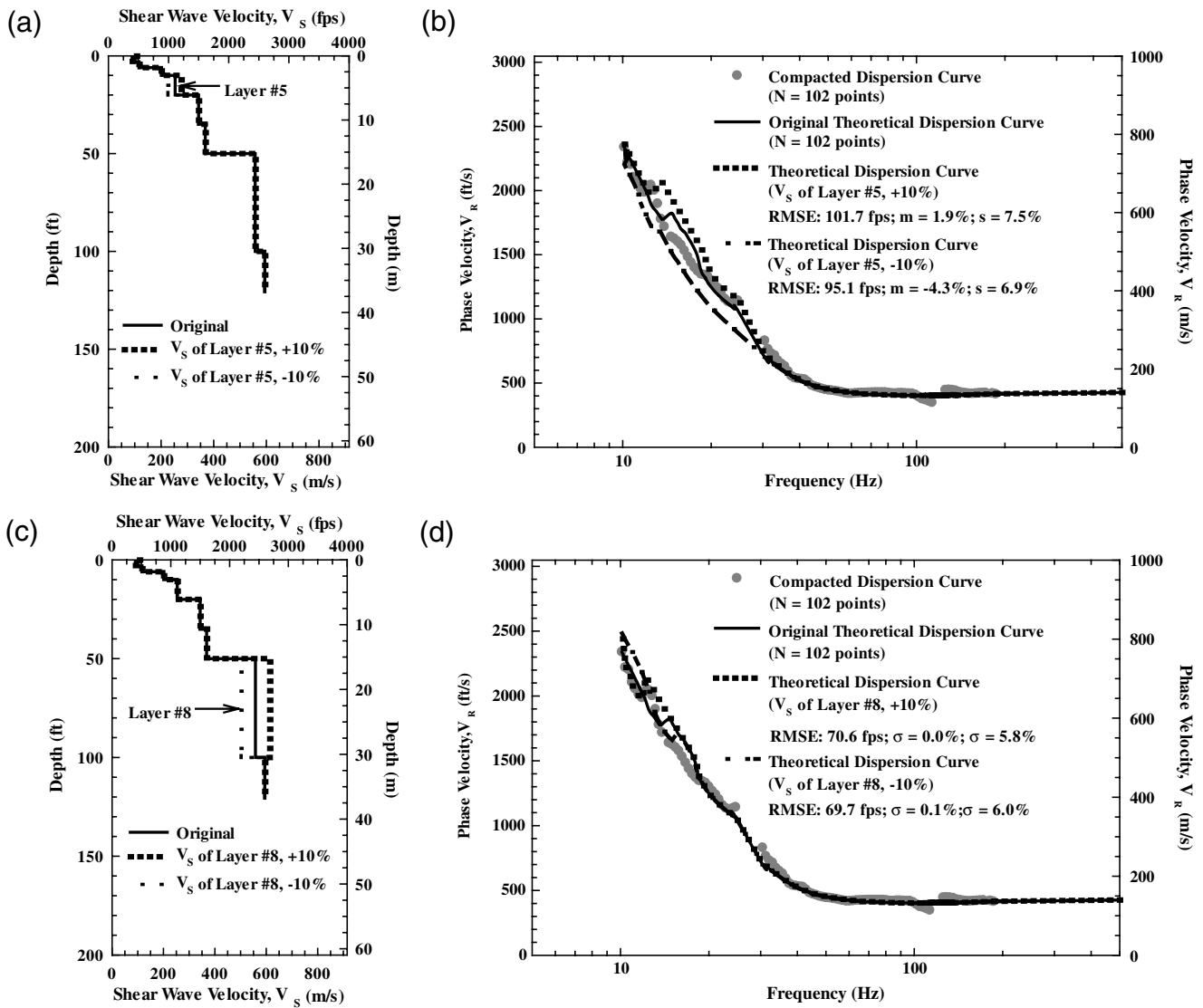
Figure 5. Parametric study of resolution in the V_S profile at the Pahoa Fire Station: (a) varying V_S of layer #5, (b) effect on the theoretical dispersion curves, (c) varying V_S of layer #8, and (d) effect on the theoretical dispersion curves.

to categorize the materials is shown in Figure 12. The trend for basalt, referred to as unweathered basalt herein, is defined by any material with $V_S \geq 2200$ ft/s at depths ≤ 75 ft and $V_S \geq 2500$ ft/s at depths > 75 ft (essentially an NEHRP B material). The trends compared with other materials are based on V_S-depth relationships of medium dense sand and dense gravel (Menq, 2003). The sand and gravel were each assumed to have relative densities of about 75% and 95%, respectively, and the water table depth was assumed at 35 ft. In terms of site classes, the V_{S30} values of the sand and gravel are 848 and 1103 ft/s, respectively, which both correspond to NEHRP site class D.

The stiffest material measured at the sites is considered to represent unweathered basalt. This material was encountered within the top 200 ft at 14 sites (Fig. 13). The V_S profiles of the unweathered basalt over the depths that they were measured along with the median, and 16th and 84th

percentile profiles are shown in Figure 13. The V_S values range from 2200 to 3200 ft/s. The coefficient of variation (COV = standard deviation[σ]/mean) and number of profiles are also shown in Figure 13. The COV is quite low (<0.15) over the depth range of about 50 to 200 ft, where at least three or more profiles were determined.

The second V_S-profile group is shown in Figure 14. This group was measured at 16 sites and is defined by: (1) a significant increase in V_S with depth in the top 50 ft and (2) median V_S values somewhat higher than dense gravel below about 5 ft but considerably less than unweathered basalt in the top 140 ft. This group is considered to represent partially weathered basalt that contains some voids, fractures, etc. This material can be seen in some shallow cuts in near-surface basalt as is present near the Waikoloa Marriott Hotel. The COV of this material decreases with depth in the top 35 ft, below which the COV is ≤ 0.12.
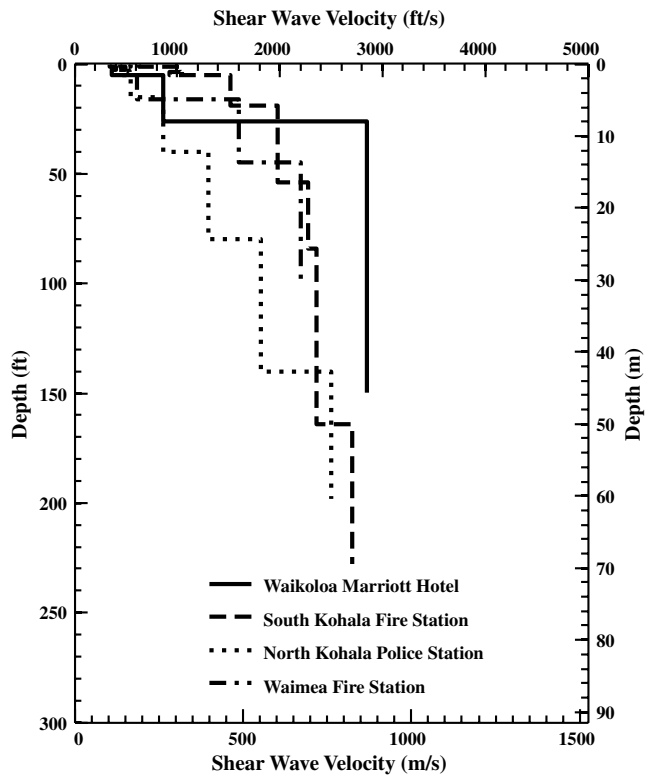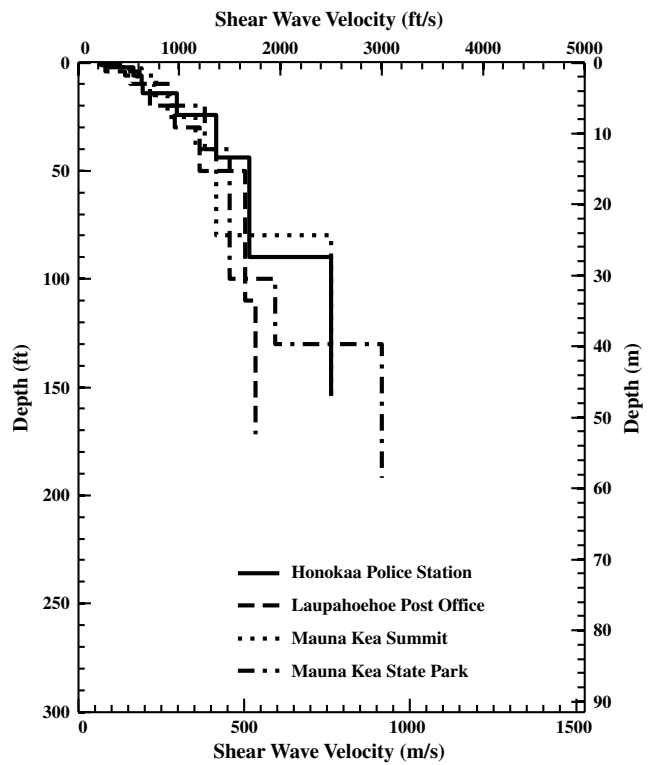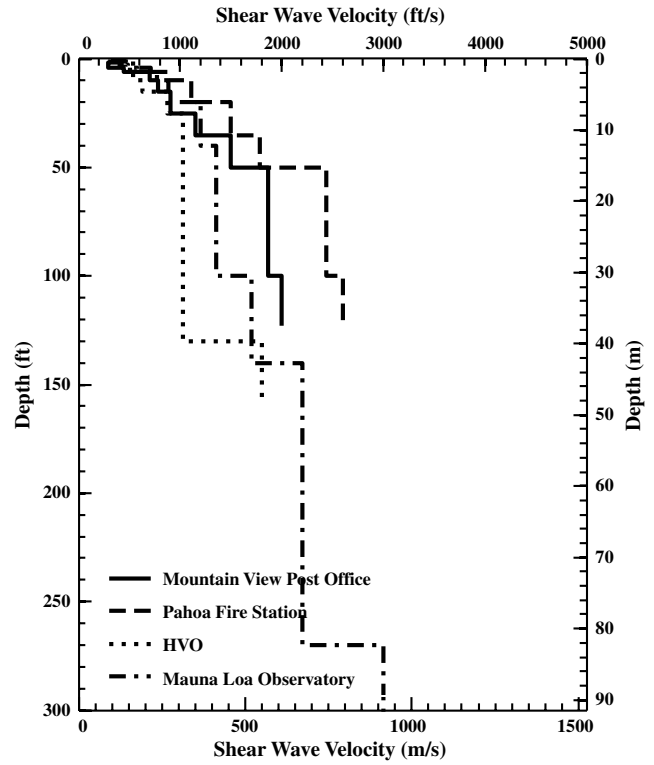
Figure 6. V_S profiles at Waikoloa Marriott Hotel, South Kohala Fire Station, North Kohala Police Station, and Waimea Fire Station.
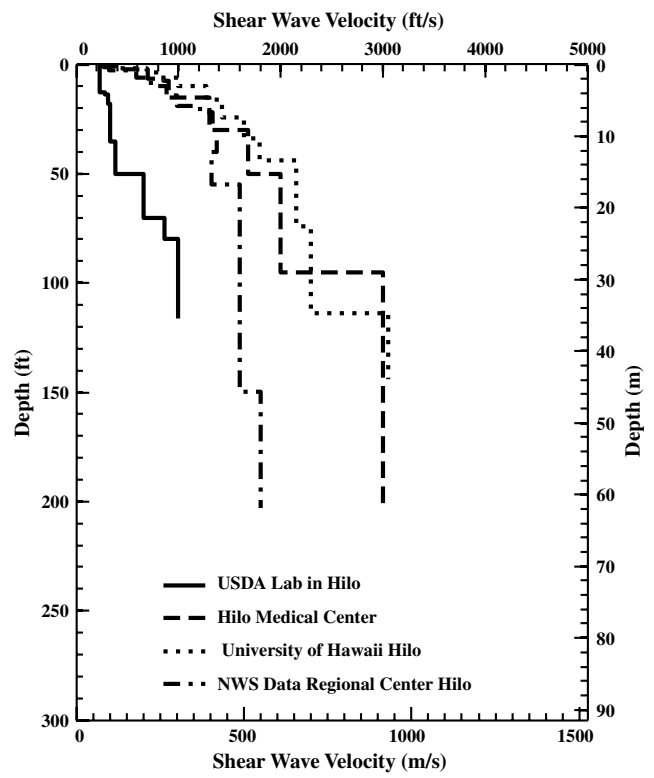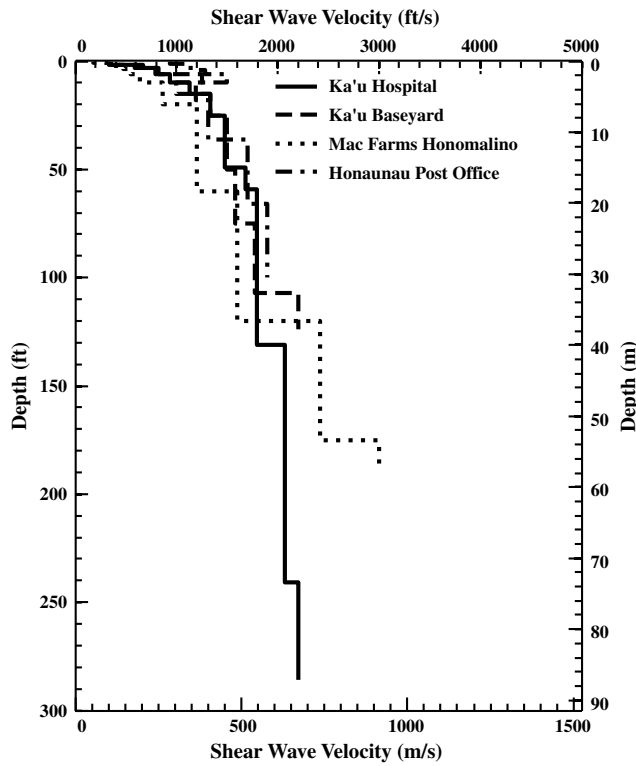

Figure 8. V_S profiles at USDA Lab in Hilo; Hilo Medical Center; University of Hawaii, Hilo; and NWS Data Regional Center, Hilo.
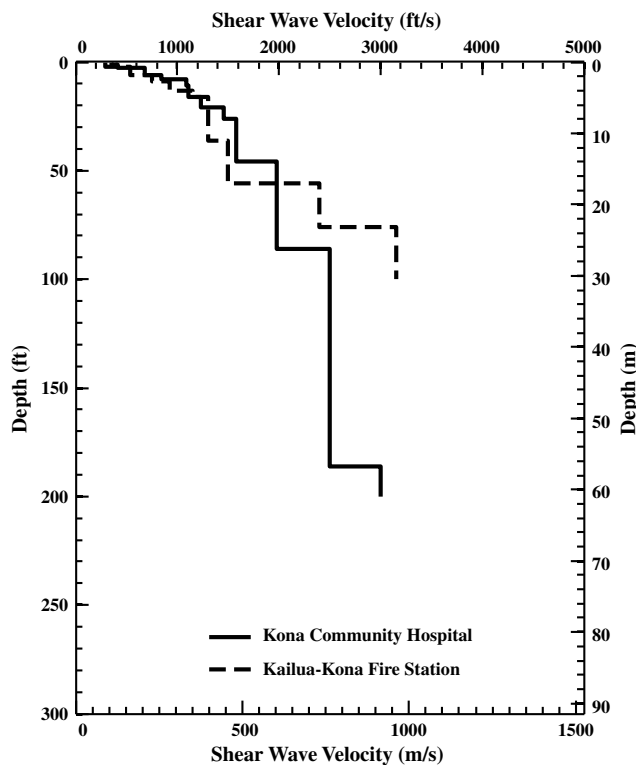

Figure 7. V_S profiles at Honokaa Police Station, Laupahoehoe Post Office, Mauna Kea Summit, and Mauna Kea State Park.

Figure 9. V_S profiles at Mountain View Post Office, Pahoa Fire Station, HVO, and Mauna Loa Observatory.

Figure 10. V_S profiles at Ka'u Hospital; Ka'u Baseyard; Mac Farms, Honomalino; and Honaunau Post Office.

Figure 11. V_S profiles at Kona Community Hospital and Kailua-Kona Fire Station.

The third and last grouping is shown in Figure 15. This group was evaluated at 16 sites and is defined by median V_S values equal to or slightly above dense gravel at depths greater than 25 ft. It is interesting to observe how closely the V_S-depth trend follows the dense gravel profile. Below about 30 ft, the COV of this material is also ≤ 0.12. This material is considered to represent stiff soil.

One or more of the three general categories of materials were encountered at 21 of the 22 sites. The thicknesses of these layers in each profile is given in Table 3. As noted previously, the soil identified in the layered profiles in Table 3 is actually the stiff soil group presented in Figure 15. At two sites, the U.S. Department of Agriculture (USDA) Laboratory and the Hawaiian Volcano Observatory (HVO), softer soil was also encountered in the profiles (Figs. 8 and 9).

Strong Motion Sites and the Kiholo Bay Earthquake

In the following, we discuss the subsurface geologic and V_S structure in the context of their possible influence on the recorded ground motions from the 2006 earthquakes. We attempted to corroborate our V_S profile results with borehole logs, but attempts to find such information were unsuccessful with the exception of one site. Site selection of the USGS strong-motion sites was not accompanied by any geotechnical site characterization, for example, drilling.

The Waikoloa Marriott Hotel was the closest strong-motion station to the 2006 earthquake and recorded a PGA of 0.19 g (Table 1). The site is underlain by 26 ft of soil and basalt with a V_S of 2850 ft/s (Fig. 6). The South Kohala Fire Station, which was installed after the 2006 earthquake, is underlain by a thin soil layer (< 5 ft) and lightly weathered basalt showing a steady V_S gradient down to at least a depth of 164 ft (Fig. 6).

The North Kohala Police Station in Kapaau and the Waimea Fire Station recorded the highest PGAs in the 2006 mainshock at more than 1 g (Table 1). Both sites show soil over weathered basalt (Fig. 6). The North Kohala Police Station V_S profile shows a strong velocity gradient in the top 200 ft. The V_S profile beneath the Waimea Fire Station shows a 16-ft-thick soil with a low V_S of 430 to 610 ft/s overlying 1600 ft/s weathered basalt (Fig. 6). Site amplification due to strong velocity contrasts and velocity gradients may account for the high PGA values. This is supported by the observation that the North Kohala Police Station also recorded the highest PGA in the Mahukona earthquake, although it was the closest strong-motion station (Table 1; Fig. 1). The Waimea Fire Station, the third closest station, also recorded a comparatively high PGA in the Mahukona event (Table 1; Fig. 1). There may be other source and path factors coming into play at these two stations including the possibility there may be a directional source effect in the 2006 mainshock ground motions because the three highest recorded PGA values recorded, North Kohala Police Station, Waimea Fire Station, and the Honokaa Police Station, are in the northernmost part of the Big Island (Fig. 1). There were

Table 3
Site Characteristics and NEHRP Site Classes of the Strong-Motion Stations on the Island of Hawaii

Station No.	Station Location	Longitude (°)	Latitude (°)	Maximum Profile Depth (ft)	V_{S30}* (ft/s)	NEHRP Site Class[†]	Geotechnical Layering Profiles Based on V_S[‡]
2810	Kailua-Kona Fire Station	−155.9923	19.6477	100	1418	C	13 ft soil/43 ft weathered basalt/basalt
2812	Ka'u Hospital, Pāhala	−155.4723	19.1999	286	1389	C	1.5 ft soil/284 ft[§] weathered basalt
2816	Pahoa Fire Station	−154.9466	19.4934	120	1497	C	10 ft soil/40 ft weathered basalt/basalt
2817	University of Hawaii, Hilo	−155.0805	19.7034	144	1615	C	1.5 ft soil/42.5 ft weathered basalt/basalt
2818	USDA Laboratory, Hilo	−155.0974	19.7277	116	437	E	70+ ft very soft soil/46+ ft soft soil
2822	Ka'u Baseyard, Waiohinu	−155.6150	19.0700	124	1365	C	1.5 ft soil/120 ft[§] weathered basalt
2824	Mauna Loa Weather Observatory	−155.5770	19.5363	318	1120	D	140 ft soil/130 ft weathered basalt/basalt
2825	Waimea Fire Station	−155.6614	20.0230	100	1375	C	16 ft soil/29 ft weathered basalt/basalt
2826	North Kohala Police Station	−155.8010	20.2300	198	1006	D	80 ft soil/60 ft weathered basalt/basalt
2829	Mauna Kea State Park	−155.5300	19.7520	192	1150	D	100 ft soil/30 ft weathered basalt/basalt
2830	Mauna Kea Summit	−155.4730	19.8260	156	1149	D	80 ft soil/basalt
2832	Honokaa Police Station	−155.4625	20.0775	154	1205	C	24 ft soil/66 ft weathered basalt/basalt
2833	Laupahoehoe Post Office	−155.2326	19.9835	172	1005	D	50 ft soil/122 ft[§] weathered basalt
2834	Mac Farms, Honomalino	−155.8680	19.1690	189	1086	D	120 ft soil/basalt
2836	Hawaiian Volcano Observatory	−155.2880	19.4200	156	890	D	130 ft soft soil/26+ ft soil
2839	Hilo Medical Center	−155.1150	19.7220	202	1430	C	15 ft soil/80 ft weathered basalt/basalt
2845	Honaunau Post Office	−155.8805	19.4174	100	1559	C	100 ft[§] weathered basalt
2846	Mountain View Post Office	−155.1083	19.5504	123	1159	D	35 ft soil/88+ ft weathered basalt
2847	Waikoloa Marriott Hotel, Anaehoomalu	−155.8870	19.9190	150	1550	C	26 ft soil/basalt
2849	Kona Community Hospital, Kea Lakekua	−155.9181	19.5215	200	1476	C	8 ft soil/78 ft weathered basalt/basalt
2852	South Kohala Fire Station, Kamuela	−155.8343	19.9464	266	1902	C	3.5 ft soil/50.5 ft weathered basalt/basalt
2853	NWS Data Regional Center, Hilo	−155.0460	19.7154	203	1176	D	203 ft[§] soil

*V_{S30} is computed from the V_S profile. The number of significant digits does not reflect the uncertainty in these values.

[†]NEHRP site class V_{S30}: A, >5000 ft/s; B, 2500 to 5000 ft/s; C, 1200 to 2500 ft/s; D, 600 to 1200 ft/s; E, <600 ft/s.

[‡]Soil refers to stiff soil category shown in Figure 14. Weathered basalt refers to material category shown in Figure 13. Basalt refers to material category shown in Figure 12.

[§]Minimum thickness.

concentrations of red- and yellow-tagged houses in Waimea and Kapaau consistent with the recorded high PGAs (Earthquake Engineering Research Institute, 2006). Site response analyses, which are beyond the scope of this study, can be performed to quantify the shallow site-response effects.

Two strong-motion stations on the north coast, Honokaa Police Station and Laupahoehoe Post Office, and two stations on Mauna Kea were surveyed (Fig. 7). All four stations recorded significant PGA values given their hypocentral distances, with the highest PGA of 0.65 *g* recorded at Honokaa Police Station at a distance of 67 km (Fig. 1; Table 1). Three of the four stations are underlain by weathered basalt. All four stations have V_S gradients in the soil and basalt with some significant impedance contrasts occurring at three of the stations. Honokaa Police Station has a jump in V_S of 1690 to 2500 ft/s at a depth of 90 ft (Fig. 7). This velocity contrast and gradient may explain the high recorded PGA value of 0.65 *g* (Fig. 1; Table 1). Mauna Kea State Park lies in a valley between Mauna Kea and Mauna Loa; this is reflected in the 100 feet of soil overlying 3000 ft/s basalt rock (Fig. 7). The V_S profile atop Mauna Kea shows a steady

increase in V_S until unweathered basalt is reached at a depth of 80 ft (Fig. 7). Shallow boreholes at one of the telescope sites drilled to a depth of 113 ft revealed fine cinders with coarser materials (ground, cobbles, and boulders) occupying the bottoms of the holes.

Four strong-motion sites were surveyed in Hilo. These sites were about 96 to 100 km from the 2006 hypocenter (Fig. 1). The PGAs are modest except at the USDA Lab (Table 1; Fig. 1). Its PGA is a factor of 3 higher than the other two strong-motion stations (Table 1). The USDA Lab is a soft soil site (NEHRP site class E) located on ash/tephra at least down to a depth of 120 ft with a V_S < 1000 ft/s (Fig. 8). In the 16 November 1983 **M** 6.6 Kaoiki earthquake, this same strong-motion site, then called the U.S. Fish and Wildlife station, also exhibited strong site amplification with factors of 5 to 6 at PGA compared with the neighboring University of Hawaii station (Buchanan-Banks, 1987). The Hilo Medical Center is reportedly also located on ash/tephra according to Sherrod *et al.* (2007), although its V_S profile indicates that the ash/tephra is not very thick if it is present at all (Fig. 8).
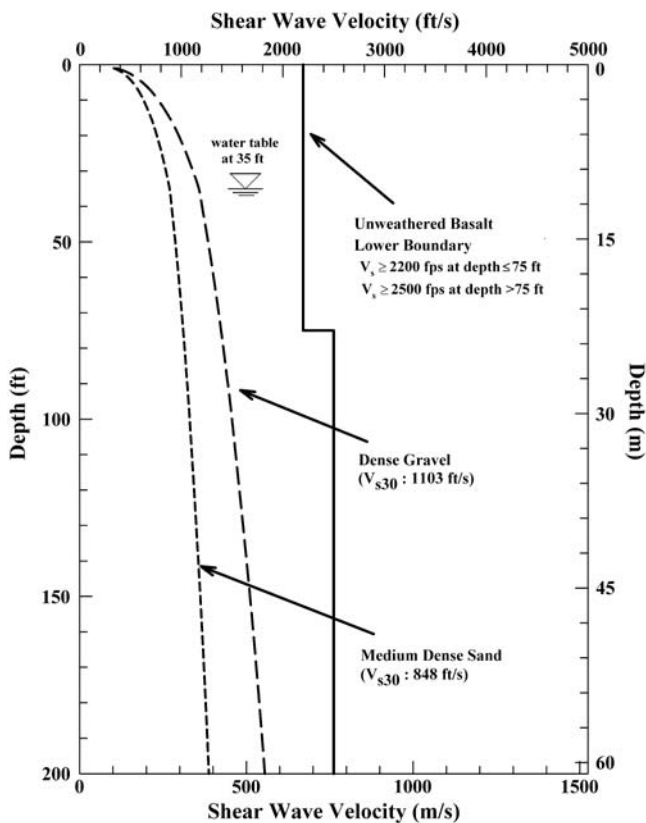
Figure 12. Template of V_S-depth relationships used to categorize geotechnical materials of the 22 sites.

Figure 9 shows the V_S profiles of the three sites in the southeastern portion of the Big Island as well as at the Mauna Loa Weather Observatory. The V_S profile at the HVO shows a thick layer of 1000 ft/s basalt with a V_S jump at a depth of about 130 ft (Fig. 9). We obtained our deepest V_S profile at the Mauna Loa Observatory (Fig. 9). Firm basalt was not reached until a depth of 270 ft. All the stations recorded modest PGAs except for the Mauna Loa Observatory, which was much closer to the 2006 earthquake (Fig. 1; Table 1).

The four stations surveyed on the southern part of the Big Island are shown in Figure 10. Moderate PGAs of 0.13 to 0.18 g were recorded at three of the sites (Fig. 1). The Mac Farms station was not operational at the time. All the sites show low to moderate V_S gradients in the basalt, although unweathered basalt is encountered at a depth of 120 ft at Mac Farms (Fig. 10). We were only able to measure to a depth of 100 ft at the Honaunau Post Office due to space limitations. The Ka'u Hospital velocity profile shows low velocity soil atop slowly increasing V_S in basalt down to a depth of 286 ft (Fig. 10).

Finally, two stations on the Kona Coast are shown in Figure 11. The Kona Community Hospital station in Kea Lakekau recorded a high PGA of 0.52 g (Fig. 1; Table 1). This was the fourth highest observed PGA, and the hospital sustained over half a million dollars of nonstructural damage in the earthquake. The hospital is located on a moderately

steep hillside, which may account for some amplification. The V_S profile shows a strong shallow gradient in the upper 45 ft with two velocity jumps at 86 and 186 ft depths (Fig. 11). This V_S profile could also account for the fairly high PGA. We had space constraints at the Kailua-Kona Fire Station and low signal quality because of what we believe is artificial fill beneath the station hence limiting the maximum depth of the survey to only 100 ft (Fig. 11). Unweathered basalt was encountered at a depth of 76 ft.

Based on observations of the strong-motion station near-surface geology and the *Geologic Map of the State of Hawaii* by Sherrod *et al.* (2007), all but the two Hilo stations are assumed to be located on basalt. However, it is obvious that the map does not adequately identify the subsurface units as discussed previously. For example, the National Weather Service (NWS) Data Regional Center in Hilo is underlain by at least 200 ft of stiff soil-like material (Table 3; Fig. 8). Given the location of the site near Hilo Bay, the soil may be largely alluvial in nature. Many of the basalt sites have soil thicknesses ranging up to more than 100 ft, for example, the HVO.

Based on the SASW survey results, all of the 22 USGS strong-motion sites are underlain by material with soil-like velocities with V_{S30} values ranging from 437 ft/s at the USDA Laboratory in Hilo (NEHRP site class E) to 1902 ft/s at the South Kohala Fire Station (NEHRP site class C) (Table 3). Twenty-one of the 22 strong-motion stations are either NEHRP site class C or D sites (Table 3). None of the strong-motion sites had rocklike V_{S30} values because of weathering, even sites where basalt outcropped at the surface, such as at the University of Hawaii at Hilo. However, note that the Waikoloa Marriott Hotel is essentially a rock site because of its high V_S in the basalt beneath the thin (26 ft) soil layer (Fig. 6). In this case, the V_{S30} of 1550 ft/s (NEHRP site class C) is misleading in terms of its potential for site amplification.

Based on the NEHRP site-class assignments, the 2006 recorded PGA values are plotted in Figure 16 against the ground-motion prediction models of Youngs *et al.* (1997) for soil and Atkinson (2010) for a V_{S30} of 1272 ft/s, the average value of the Big Island strong-motion sites. Although the 2006 data occupy a relatively narrow distance range of 39 to 118 km, they are consistent with the Atkinson (2010) ground-motion prediction curves for an **M** 6.9 at a depth of 38.9 km, as might be expected given Atkinson (2010) used these data in the development of her model. The PGAs, however, show a large variability spanning the range encompassed by ±one sigma (Fig. 16). The majority of the PGA values are above the median relationship of Youngs *et al.* (1997); hence, the hazard from deep earthquakes is probably underestimated in the 2001 USGS Hawaii hazard maps. Note the USDA Laboratory site (NEHRP site class E) exhibits the highest PGA of all stations in its distance range (Fig. 16), reflecting the strong amplification at this site due to the underlying ash deposits.
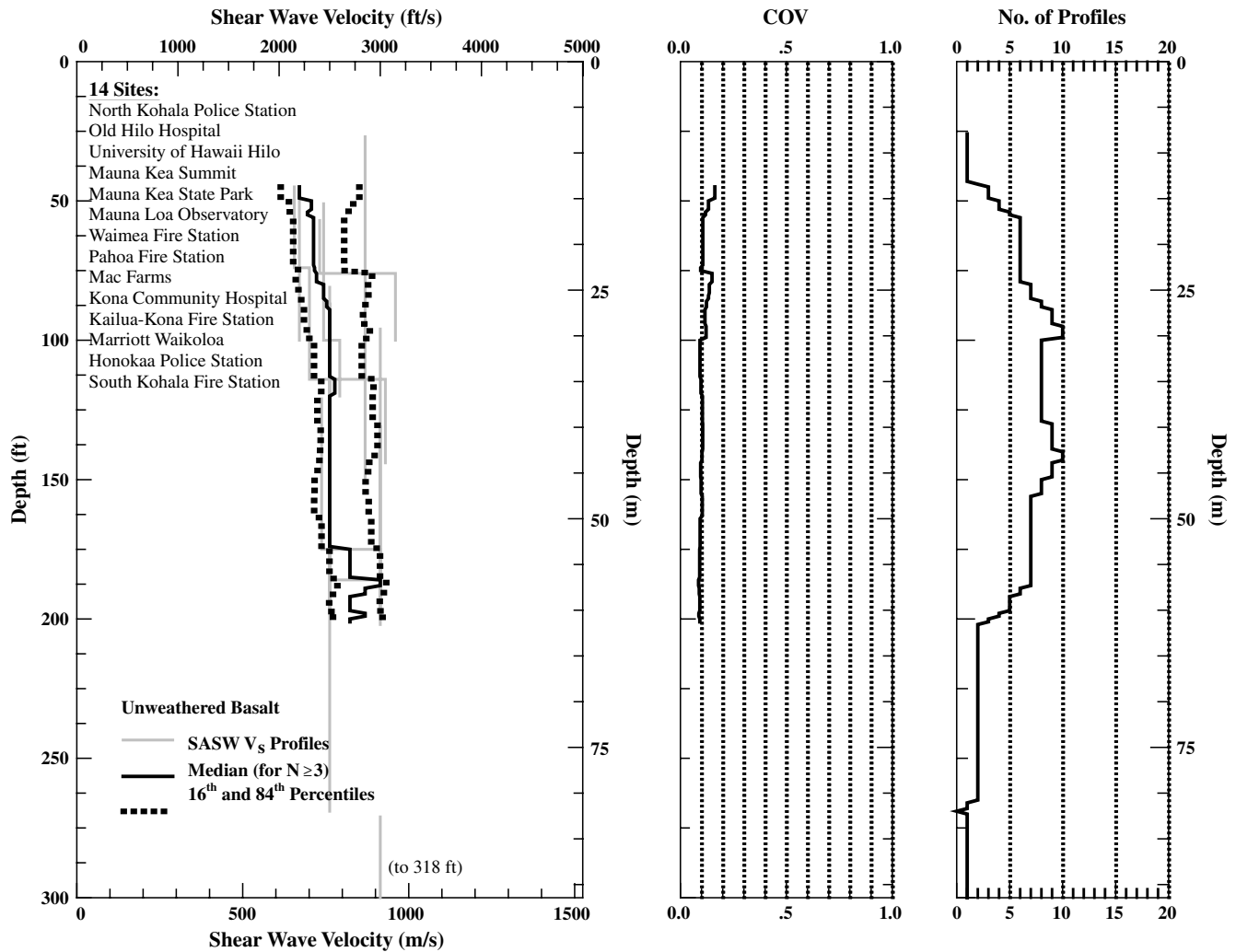
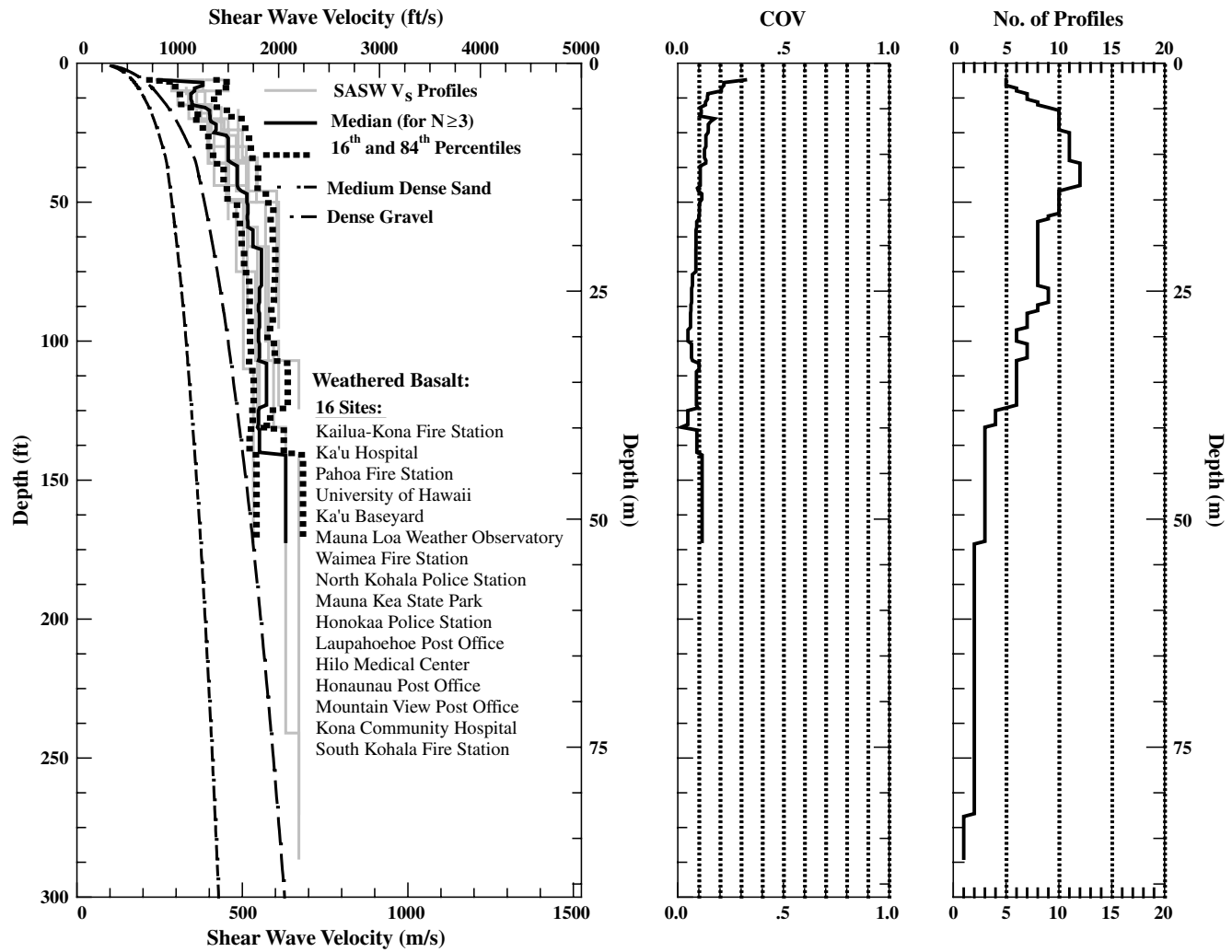**Figure 13.**   Statistical analysis of the unweathered basalt V_S profiles.

Figure 17 compares the maximum recorded PGA versus V_{S30} and hypocentral distance. Within most of the 10-km distance bin, there is no apparent trend of increasing PGA with decreasing V_{S30}. This is most obvious in the 50-, 60-, and 90-km distance bins (Fig. 17). The high PGA values recorded by the Waimea Fire Station (#2826) and North Kohala Police Station (#2825) are only marginally different, yet they are in different NEHRP site classes due to their differing V_{S30} values (Fig. 17). Hence, there must be other factors including source, path, and/or site effects beneath a depth of 30 m that are controlling the level of PGAs for this earthquake. In the 80 km distance bin, the USDA Laboratory site with its low V_{S30} shows the highest PGA as also indicated in Figure 16.

Development of NEHRP Site-Class Map

The first NEHRP site-class map for the Big Island was developed in 2006 by URS Corporation (see Data and Resources), but because no V_S data were available for this desktop study, it was based solely on the *Geologic Map of*

the Island of Hawaii by Wolfe and Morris (1996), updated by Sherrod *et al.* (2007), and limited geotechnical borehole data. As a result, based on the assumption that basalt would be rocklike, the map portrayed nearly all the Big Island as NEHRP site class B. The recent SASW surveys show this not to be true; rather, the 19 sites on basalt are classified as NEHRP site classes C or D (Table 3). Thus, we have developed a new 1:100,000-scale map of NEHRP site class for the Big Island. This new map, based largely on the SASW measurements, the 1:100,000-scale geologic mapping by Sherrod *et al.* (2007), and our past experience in measuring V_S in similar materials (e.g., Wong and Silva, 2006; Wong *et al.*, 2011) is shown in Figure 18.

To produce the NEHRP site-class map, V_{S30} measurements are related to geologic map units, then the geologic map is used as the basis for the NEHRP site-class map. The locations of SASW measurements were intersected with the most recent geologic map (Sherrod *et al.*, 2007) in a geographic information system. All geologic map units in the map were then grouped into categories based on differences in V_{S30} measurements, for the units in which SASW data

Figure 14. Statistical analysis of the partially weathered basalt V_S profiles.

were collected, and based on assumed similarities in map units for the units in which SASW data were not collected. Table 2 shows the map unit groups, the number of SASW measurements for each group, and general statistics describing the suite of SASW measurements for each group. As is common for geological, geotechnical, and geophysical data, the data are not normally distributed (Fig. 19), and the variability between groups based on geologic map units can be as large as the variability within groups. However, the only map unit group for which sufficient SASW data are available to provide a reasonably robust characterization are basalts. Limited SASW data were collected in the other map unit groups (Table 2).

Areas of basalt (much of the island) should be considered NEHRP site class C or D in the new map (Knudsen *et al.*, 2008). The 19 SASW-sampled sites cover a range of basaltic rock conditions, and the geologic map includes a range of units classified as basalt, including lava flows, scoria cones, littoral deposits, spatter or tuff cones, cinder cones, and lava domes. The median value for these V_{S30} estimates is 1365 ft/s with a standard deviation of 257 ft/s and a log

mean of 1312 ft/s. The variability in V_{S30} measurements in areas mapped as basalt may be a reflection of the wide range of map units lumped in the basalt map group. The variation may also be a result of differences in weathering profiles or in stratigraphy. Some areas mapped as basalt may be underlain by consistently hard basalt with few voids, whereas others may be underlain by layers of void-rich basalt interlayered with tephra layers. Clearly the V_S profile in these two situations would be different, although the geologic map would not indicate such differences.

To attempt to subdivide areas mapped as basalt on the NEHRP site-class map, a number of parameters were tested to see if they controlled V_{S30} values. Among the parameters evaluated were age of map unit, source volcano, shield versus postshield volcano, and elevation. Perhaps the relatively small sample size ($n = 19$) does not provide sufficient data for a statistically valid comparison, but preliminary analyses suggest that none of these parameters correlate well with V_{S30}.

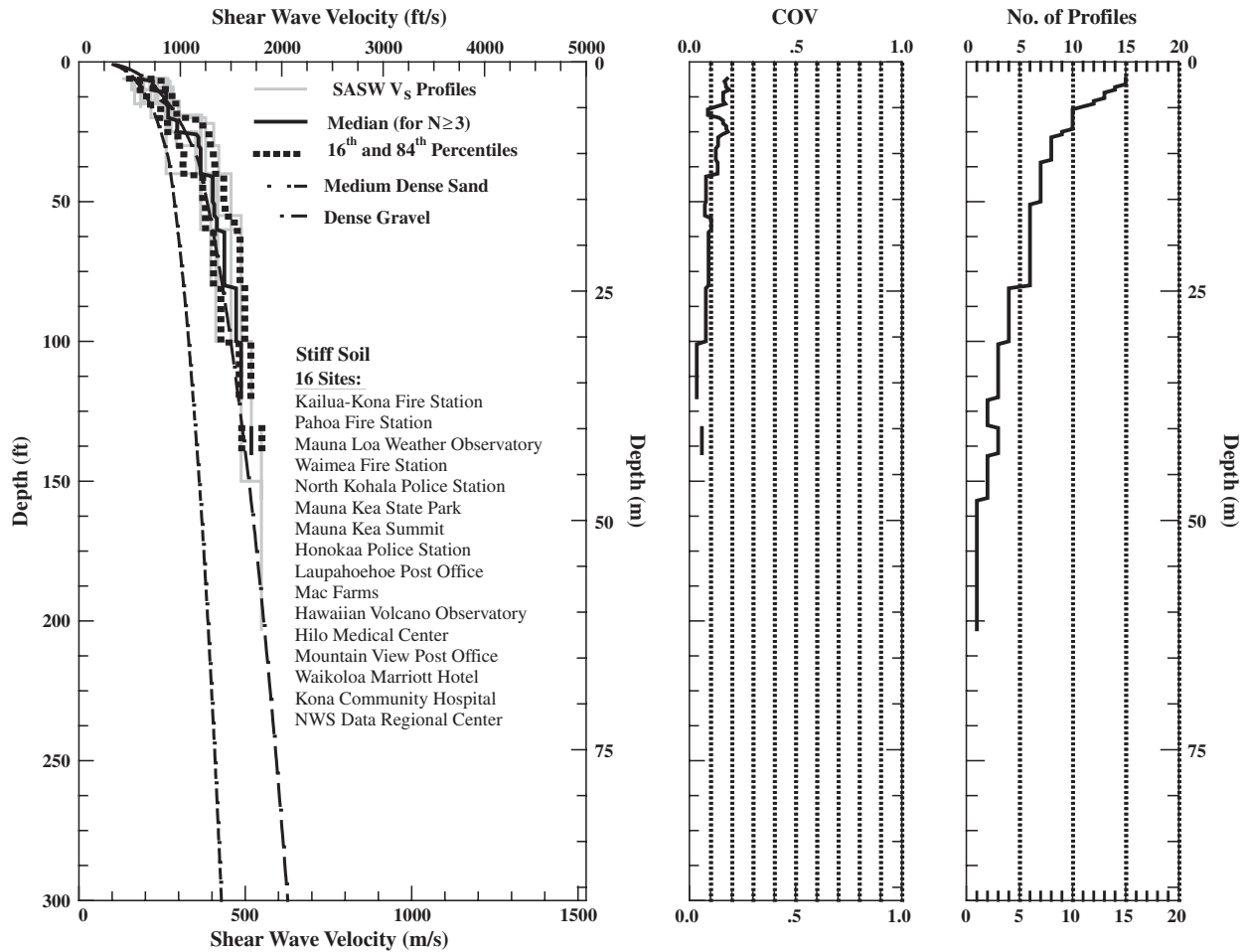Other geologic map unit groups used in generating the NEHRP site-class map, for which only one or two V_{S30}

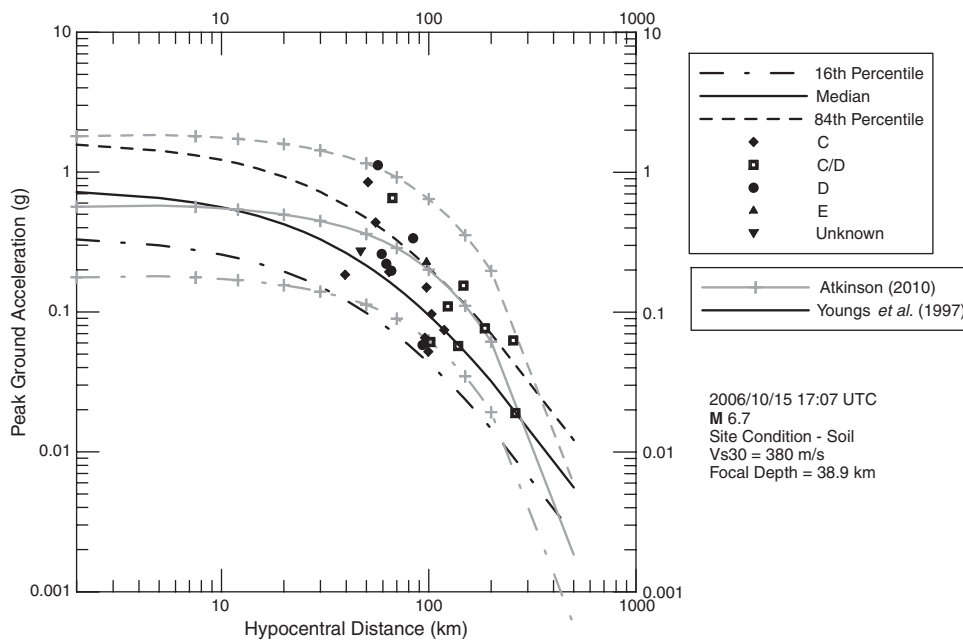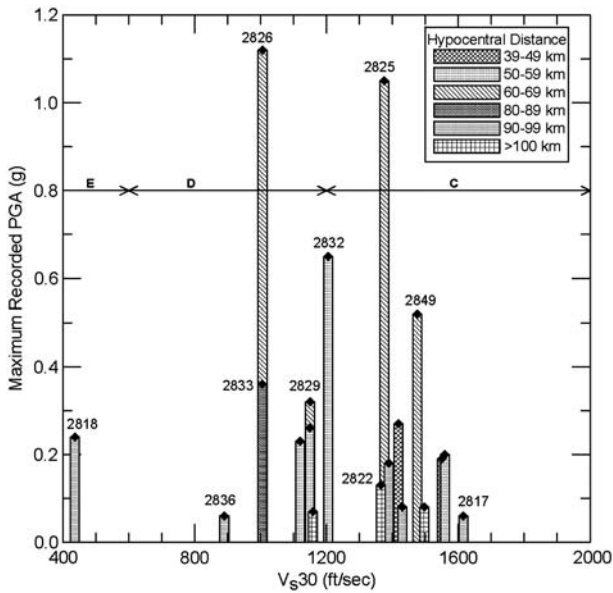**Figure 15.**   Statistical analysis of the stiff soil V_S profiles.

Figure 16.   Comparison of Youngs *et al.* (1997) and Atkinson (2010) ground motion prediction models for soil (V_{S30} 1272 ft/s) and the recorded PGAs from the 2006 **M** 6.7 Kiholo Bay earthquake.

Figure 17. Maximum PGA versus V_{S30}. Stations are binned by hypocentral distance. Selected stations are labeled (see Table 3). NEHRP site classes C, D, and E in terms of V_{S30} are also shown.

estimates were made from SASW data, include alluvium ($n = 1$), ash/tephra ($n = 2$), and artificial fill ($n = 2$). These map unit groups were assigned NEHRP D or E, based on the available data and on a rudimentary understanding of the typical properties of these kinds of deposits (Table 2). Geologic deposits for which SASW data are not available include sand dunes, landslide deposits, and glacial deposits. The NEHRP site classes "D" or "C or D" were assumed for these units and used in the NEHRP site-class map (Fig. 18). Clearly, values for these parts of the site map are not well constrained.

Conclusions

Spectral-analysis-of-surface-waves surveys were performed at the 22 free-field strong-motion sites of the USGS Hawaii Strong Motion Network on the Big Island. V_S profiles reaching depths ranging from 100 to 318 ft were obtained. Most of the surveyed sites were located on basalt or weathered soil atop basalt and correspond to NEHRP site classes C or D. A qualitative examination of the V_S profiles beneath the strong-motion sites suggests that the site effects
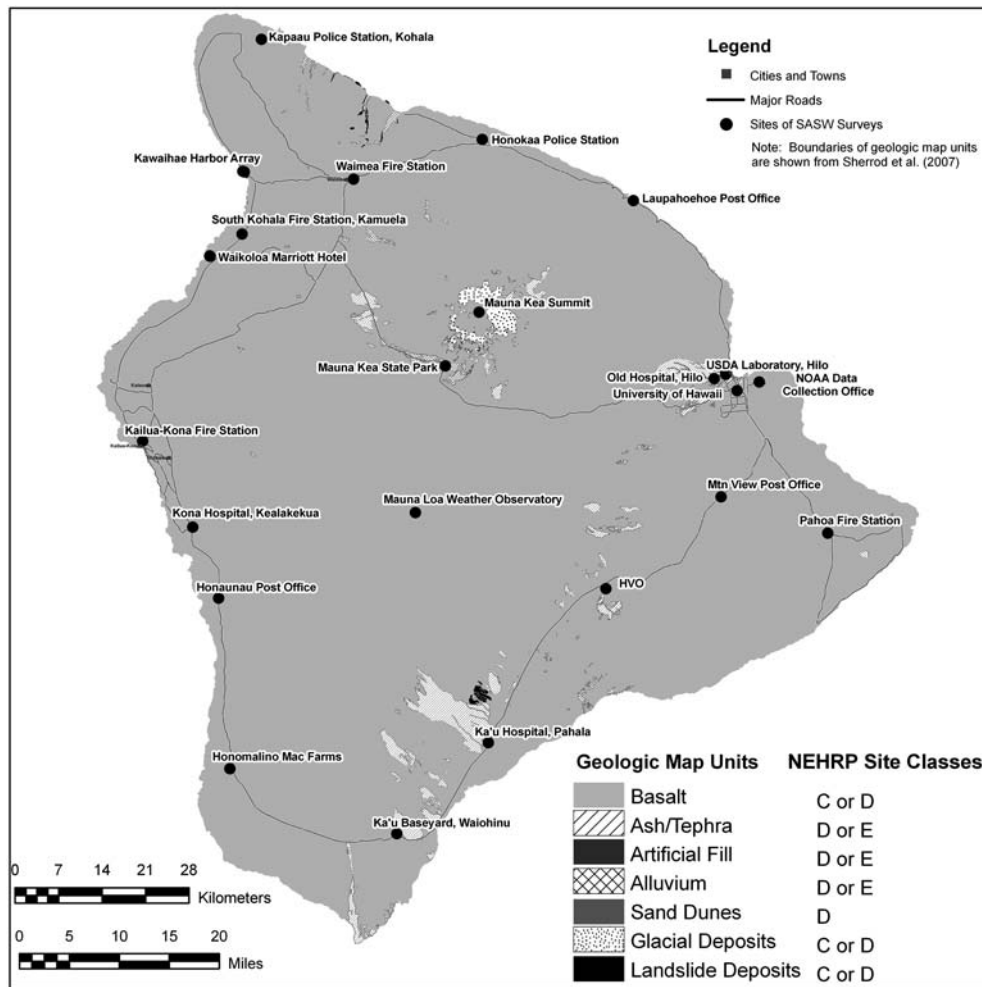
Figure 18. New NEHRP site-class map for the island of Hawaii. Geologic map units from Sherrod *et al.* (2007).
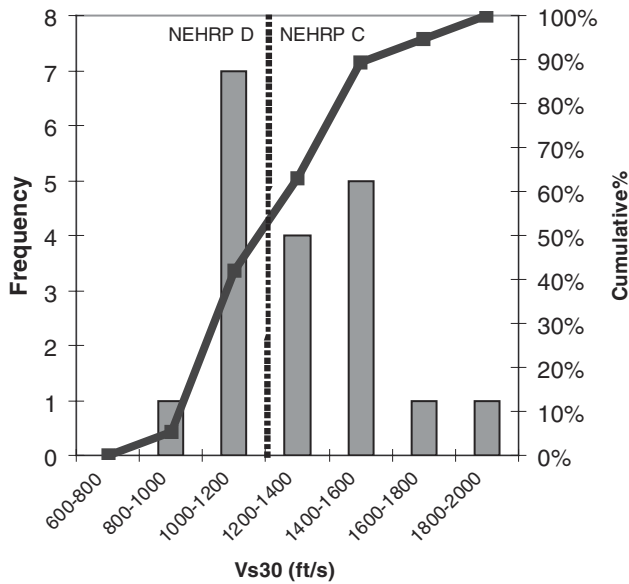
Figure 19. Distribution of V_{S30} for the 19 USGS strong-motion sites underlain by basalt as characterized by Sherrod *et al.* (2007). See Table 2 for statistics.

could be largely responsible for the observed ground motions in the 2006 Kiholo Bay mainshock, although other source and path factors may be coming into play.

The new NEHRP site-class map provides a more realistic foundation for ground-shaking hazard assessments than the previous map (URS Corporation; see Data and Resources), because it is based on SASW-based estimates of V_{S30}. However, the limited number of SASW tests, the variability in V_{S30} values for geologic map unit groups, and the absence of SASW data for several of the map unit groups, show that more surveys and analyses would reduce the uncertainty in the map. Site-specific seismic hazard evaluations should be based on *in situ* V_S surveys given the variability of V_S we have observed on the Big Island.

Data Resources

Data from the USGS Hawaiian strong-motion network are available at http://nsmp.wr.usgs.gov (last accessed July 2011). The URS (2006) publication, "Developing a Hawaii NEHRP site class map for use in HAZUS-MH earthquake loss estimation, draft technical report for FEMA," U.S. Department of Homeland Security, is available only upon request to URS Corporation. The raw data from the SASW survey measurements and the template V_S profiles can be obtained from the second author. The SASW-derived V_S profiles are available from the first author.

Acknowledgments

References

Atkinson, G. M. (2010). Ground motion prediction equations for Hawaii from a referenced empirical approach, *Bull. Seismol. Soc. Am.* **100,** 751–761.

Buchanan-Banks, J. M. (1987). Structural damage and ground failures from the November 16, 1983 Kaoiki earthquake, island of Hawaii, *U.S. Geol. Surv. Profess. Pap. 1350*, 1187–1220.

Earthquake Engineering Research Institute (EERI) (2006). Compilation of observations of the October 15, 2006 Kiholo Bay (M_w 6.7) and Mahukona (M_w 6.0) earthquakes, Hawai'i, Chock, Gary ed., 53 pp.

Joh, S.-H. (1996). Advances in interpretation and analysis techniques for spectral-analysis-of-surface-waves (SASW) measurements, *Ph.D. Thesis*, University of Texas, Austin, Texas, 240 pp.

Klein, F. W., A. D. Frankel, C. S. Mueller, R. L. Wesson, and P. G. Okubo (2001). Seismic hazard in Hawaii: High rate of large earthquakes and probabilistic ground-motion maps, *Bull. Seismol. Soc. Am.* **91,** 479–498.

Knudsen, K. L., I. G. Wong, and F. Terra (2008). A NEHRP site class map for the Island of Hawaii (abs.), *Eos Trans. Am. Geophys. Union* **89**.

Lin, Y.-C., and K. H. Stokoe II (2008). Variability in V_S profiles and consistency between seismic profiling methods: A case study in Imperial Valley, California, *Proc. of the 3rd International Conf. on Site Characterization, ISC'3*, A.-B. Huang and P. W. Mayne (Editors), Taipei, Taiwan, *1–4 April, 3*, 218–224.

Menq, F. Y. (2003). Dynamic properties of sandy and gravelly soils, *Ph.D. Thesis*, University of Texas, Austin, Texas, 364 pp.

Munson, C. G., and C. H. Thurber (1997). Analysis of the attenuation of strong ground motion on the island of Hawaii, *Bull. Seismol. Soc. Am.* **87,** 945–960.

Porter, S. C. (1997). Late Pleistocene eolian sediments related to pyroclastic eruptions of Mauna Kea volcano, Hawaii, *Quaternary Research* **47,** 261–276.

Rosenblad, B. L., K. H. Stokoe, E. M. Rathje, and M. Darendeli (2001). Characterization of strong motion stations shaken by the Kocaeli and Duzce earthquake in Turkey, *Geotechnical Engineering Report GR01-1*, Geotechnical Engineering Center, University of Texas, Austin, Texas, 142 pp.

Sherrod, D. R., J. M. Sinton, and S. E. Watkins (2007). Geologic map of the State of Hawaii (sheet 8-Island of Hawaii), *U.S. Geol. Surv. Open-File Rept. 2007-1089*, scale 1:100,000.

Stephens, C. D., W. U. Savage, P. G. Okubo, and E. C. Anjal (2007). Update on strong-motion recordings of the October 15, 2006 **M** 6.7 Kiholo Bay, Hawaii, earthquake sequence (abs.), *Seismol. Res. Lett.* **78,** 303–304.

Stokoe, K. H., S. H. Joh II, and R. D. Woods (2004). Some contributions of *in situ* geophysical measurements to solving geotechnical engineering problems, *Proc. of the 2nd International Conf. on Site Characterization, ISC'2*, A. Viana da Fonseca and P. W. Mayne (Editors), Porto, Portugal, 19–22 September, 1, 97–132.

Stokoe, K. H., B. L. Rosenblad II, J. A. Bay, B. Redpath, J. G. Diehl, R. Steller, I. G. Wong, P. A. Thomas, and M. Luebbers (2003).

Comparison of V_S profiles from three seismic methods at Yucca Mountain, in *Soil and Rock America 2003*, P. J. Culligan, H. H. Einstein, and A. J. Whittle (editors), Verlag Glückauf GMBH, Cambridge Massachusetts, 22–26 June, 1, 299–306.

Stokoe, K. H., S. G. Wright II, J. A. Bay, and J. M. Roesset (1994). Characterization of geotechnical sites by SASW method, in *Technical Report—Geophysical Characterization of Sites*, R. D. Woods (editor), prepared by ISSMFE Technical Committee 10, Oxford Publishers, *13th International Conf. on Soil Mechanics and Foundation Engineering*, New Delhi, India, 5–10 January, 15–26.

Wolfe, E. W., and J. Morris (1996). Geologic map of the Island of Hawaii, *U.S. Geol. Surv. Miscellaneous Investigations Series I-2524-A*, scale 1:100,000.

Wong, I., and W. Silva (2006). The importance of *in situ* shear-wave velocity measurements in developing urban and regional earthquake hazard maps, *Proc. of the 19th Annual Symposium on the Application of Geophysics to Engineering and Environmental Problems*, 2–6 April 2006, 1304–1315 (CD ROM).

Wong, I., K. Stokoe, B. Cox, F.-Y. Menq, C. Hoffpauir, and P. Okubo (2008). Shear-wave velocity profiling of the USGS strong motion stations on the Island of Hawaii (abs.), *Seismol. Res. Lett.* **79,** 339.

Wong, I. G., K. H. Stokoe II, B. R. Cox, Y-C. Lin, and F-Y. Menq (2011). Shear-wave velocity profiling of strong motion sites that recorded the 2001 Nisqually, Washington, earthquake, *Earthquake Spectra* **27,** 183–212.

Youngs, R. R., S.-J. Chiou, W. J. Silva, and J. R. Humphrey (1997). Strong ground motion attenuation relationships for subduction zone earthquakes, *Seismol. Res. Lett.* **68,** 58–73.

URS Corporation
Seismic Hazards Group
1333 Broadway, Suite 800
Oakland, California 94612
    (I.G.W., K.L.K., F.T.)

University of Texas at Austin
Geotechnical Engineering Center
1 University Station C1793
Austin, Texas 78712
    (K.H.S., J.Y., Y.-C.L.)

University of Arkansas
Department of Civil Engineering
4190 Bell Engineering Center 4155A
Fayetteville, Arkansas 72701
    (B.R.C.)

USGS Hawaiian Volcano Observatory
Hawaii National Park
Hawaii 96718
    (P.O.)